The Impact of African and Brazilian ZIKV isolates on neuroprogenitors

Loraine Campanati[1, *], Luiza M. Higa[2, *], Rodrigo Delvecchio[2], Paula Pezzuto[2], Ana Luiza Valadão[2], Fábio L. Monteiro[2], Grasiella M.Ventura[3], Carla Veríssimo[1], Ana M. Bispo De Filippis[4], Renato S. Aguiar[2], Amilcar Tanuri[2].

1- Laboratório de Morfogênese Celular, Instituto de Ciências Biomédicas, Universidade Federal do Rio de Janeiro.

2- Laboratório de Virologia Molecular, Departamento de Genética, Instituto de Biologia, Universidade Federal do Rio de Janeiro.

3- Unidade de Microscopia Confocal, Instituto de Ciências Biomédicas, Universidade Federal do Rio de Janeiro.

4- Laboratório de Flavivírus, Instituto Oswaldo Cruz, Fundação Oswaldo Cruz, Rio de Janeiro, Brazil

*These authors contributed equally to this work

In the last few months, an overwhelming number of people have been exposed to the Zika virus (ZIKV) all over South and Central America. Healthcare professionals noticed an alarming surge of fetuses diagnosed with microcephaly and several other brain malformations from mothers who showed signs of the disease during pregnancy[1-3]. There was also an increase in the number of reported cases of Guillain-Barré syndrome that are now associated with the Zika epidemics[4]. Sequencing and phylogenetic data from our group showed that isolates from Brazilian patients are 97-100% identical to the virus isolated from the outbreak in the French Polynesia, while showing 87-90% identity to African isolates[5]. To date, there is no report of either cases of congenital abnormalities or Guillain-Barré syndrome in African countries, pointing to the possibility that differences in the genome sequences of these viral strains may be associated to different clinical outcomes. In this work we showed, *in vitro*, that the Brazilian virus has a greater impact

on murine neuronal progenitors and neurons than the African strain MR766. We found that the Brazilian isolate more pronouncedly inhibits neurite extension from neurospheres, alters their differentiation potential and causes neurons to have less and shorter processes. Comparing both lineages using a panel of inflammatory cytokines, we showed, with human neuroblastoma cells, that ZIKV induces the production of several inflammatory and chemotactic cytokines and once again, the Brazilian isolate had a more significant impact in immune activation response. Although much more needs to be studied regarding the association of ZIKV infection and brain damage during development, our study sheds some light into the differences between African and American lineages and the mechanisms by which the virus may be affecting neurogenesis.

Main text

Very recent evidences correlate ZIKV infection to damage to the nervous system and there is a lack of information about the effects of both African and Brazilian isolates on neural cells[1,5]. When the polyprotein sequence from prototypic African ZIKV isolate MR766 was compared to the pandemic strain circulating in South America, we found an overall identity of 96.4 % and a 98.4% of similarity. When the structural and non-structural proteins of the South American isolate ZIKV Br 3189[5] is compared to MR766, there are 129 amino acids changes. Most of these substitutions are conservative and are mainly located in the envelope and NS4b viral proteins. In this work, we sought to comparatively investigate the outcomes of these two ZIKV lineages infections in different cell types.

Pathogenesis of microcephaly involves the disrupted regulation of the number of neurons produced by neuronal precursors[6]. Congenital Cytomegalovirus infection is known to lead to microcephaly by the inhibition of NSCs differentiation into neurons[7]. It is also established that flaviviruses infect neurons as well as glial cells[8,9] and that the Japanese encephalitis virus (JEV) infects neural stem cells leading to changes in their differentiation potential[10,11]. Here, using both Brazilian and African isolates of ZIKV, we infected neurospheres derived from murine E14 cortex, SH-SY5Y cells (human neuroblastoma cell line permissive to viruses), mouse cortical neural stem cells (NSCs) and neurons. Neurospheres, grown in Neurobasal medium supplemented with B27 were infected to up to 72h. We found that infection with both isolates decreased the area of spheres (Fig 1): ZIKV Br by 21% (3099 ± 211 μm^2), while MR766 had a less pronounced effect: 9% (3548 ± 203 μm^2). By phase contrast and confocal microscopy, mock-infected neurospheres (3907 ± 239 μm^2) showed exuberant thin cell processes (Fig. 1a) with positive staining for microtubule-associated protein 2 (Map2), a marker of neuronal differentiation (Fig. 1b). MR766 infected neurospheres also exhibited $Map2^+$ neurites, (Figs. 1c, 1d) although we noticed that in small neurospheres projections were often misshapen (Fig. S5). ZIKV Br infection greatly reduced the amount of $Map2^+$ cellular processes and we noticed $Map2^-$ cells with progenitor-like morphology migrating out of the spheres (Fig. 1e, 1f and additional data in Fig S4).

Differentiated cortical neurons were also infected with both isolates (Fig.2). Mock infected neurons (Fig.2a) showed long, intricate neurites growing out of the cell body, while MR766 and ZIKV Br infected cells show less and simpler processes (Figs. 2b, 2c). No infection was observed in differentiated neuronal cells with both MR766 and ZIKV

Br evidenced by IF using an anti-Flavivirus 4G2 antibody (Supp. methods), but rather the labeling of cells with shorter $Map2^{+}$ processes (Figs. 2b, green).

In neurospheres, using a higher viral load of MR766, we observed $Map2^{low}$ cells stained with 4G2 (Figs. 2d-e), mainly in the periphery of the spheres. Only rarely, we observed double-labeled (Map2/4G2) processes leaving the neurospheres (Fig. S3), which is in accordance with data published recently showing that the ZIKV infection rate in human neurons is low [12].

We performed qPCR targeting ZIKV genome (supp. methods) and verified intracellular presence of total viral RNA and negative-sense RNA strand, the template for viral genome replication, revealing that all cell types were permissive and productively infected by both viruses (Supp. table 1). MR766 infection of human NSCs was described recently[12] and here we showed that viral replication in rodent NSCs was more effective with ZIKV Br than with ZIKV MR766. In contrast, MR766 produced higher levels of intracellular RNA than ZIKV Br in neurospheres enriched in neuronal progenitors and SH-SY5Y cells, whose culture is known to have "neuroblast-like" cells[13]. Taken together, these results show that both viruses are neurotropic, but have different replicative patterns depending on the differentiation status of the host cell, ZIKV Br being more replicative in undifferentiated cells than ZIKV MR766.

Interestingly, even with lower levels of ZIKV Br replication in neurospheres, we observed more pronounced effects in neurite outgrowth by this isolate than when compared to ZIKV MR766. This result suggests a stronger impact in neuronal differentiation induced by our Brazilian isolate, which can be of great importance when

one takes into account the outcome of infections in earlier phases of the nervous system development.

Others flavivirus infection are associated to elevated levels of proinflammatory cytokines and chemokines that contribute to neuropathogenesis[10,14-16]. To further compare the immune activation caused by both viruses, we investigated the cytokine profile in the supernatant of SH-SY5Y cells infected with MR766 and ZIKV Br and found a significant increase of several cytokines when compared to mock infected cells (Supplementary Table 2). Of note, two pro-inflammatory cytokines IL-1β and TNFα, four chemokines IL-8, IP-10, RANTES, Eotaxin and growth factors FGF2 and G-CSF were detected in higher concentration in the supernatant of ZIKV Br infected cells. Unlike expected, most of the cytokines were not modulated by MR766 infection, except the pro-inflammatory IL-6 that was tightly down-regulated (Fig.3). IL-1β and TNFα act as potent mediators of neuronal death in several neurological disorders, West Nile virus and JEV infections[17]. In neuroprogenitor cells it has been shown that IL-1β decreases cell proliferation while TNFα induces cell death via caspase-8-mediated apoptosis[18]. Moreover, high levels of IL-8 has been shown to induce pro-apoptotic proteins and cell death in cultured neurons [19]. RANTES levels is associated with viral encephalites and can be induce by NF-kB activation via IL-1β and TNFα stimulus in glial cells[15,20]. IP-10 is a chemokine induced by viral infection in astrocytes that can regulate IFNγ levels[21]. In our experiment, IFNγ had a slight increase despite of IP-10 levels. Eotaxin high levels are also associated to neurodegenerative disorder[22]. The growth factors FGF2 and G-CSF are important cytokines involved in NSC proliferation and neurogenesis providing neuroprotection and decreasing apoptosis[23,24]. Cytokine profile analysis can help us understand how immune

response stimulated by ZIKV infection could disturb neuroprogenitor cells and contribute to the higher numbers of microcephaly and encephalitis cases described in South America and Asian countries with ZIKV outbreaks[25].

Retrospective analysis of the recent Zika outbreak in French Polynesia provided evidence associating ZIKV infection to the development of Guillain-Barré syndrome. Moreover, statistical analyses now support the correlation of congenital infection and microcephaly cases [4,26].

Recently, ZIKV particles were identified in the brain tissue of a fetus, diagnosed with microcephaly and other brain damages[1]. Overall, it is becoming increasingly clear that Zika virus is as highly neurotropic as other flaviviruses. It is not known, however, to which extent the Brazilian strain infectivity is different from the African strain. The work presented here indicates that the ZIKV lineage circulating in South America, belonging to Asian lineage, gained a novel capacity of altering neuroprogenitor cells when compared to the isolate from the Zika forest in Uganda in 1947. In fact, several critical differences were found between these two lineages. The main differences are located in two critical points of the viral genome. The first main modification acquired by ZIKV Br, is a new, canonical N-Linked glycosylation site located at position 153 of the envelope protein and other cluster of mutation is located at the cytoplasmic loop of NS4b protein. This site is implicated in the induction of membrane synthesis and replication competence in Dengue virus[27], as well as signal transduction related to malignant transformation in HCV[28] (Supplementary Figures 1 and 2). These unique properties of the Asian lineage showed here could certainly impact the field of vaccine and antiviral development to this new pathogenic agent.

Figure legends

Figure 1: Infection with ZIKV Br inhibits Map2 process elongation and decreases the area of neurospheres. Mock infected neurospheres extend long, $Map2^{+}$ processes (a,b), while MR766 infected suffered little with viral infection (c,d). Spheres infected with ZIKV Br (e,f) showed more drastic effect and only few neurites were seen. Mean area of the neurospheres in μm^2 (g) ± s.e.m. ***p<0,001; *p<0,05; Student's t test.

Figure 2: ZIKV infection decreases neuronal branching in culture. Neurons infected with both ZIKV isolates showed less branching (b, MR766; c, ZIKV Br) than Mock infected cells. ZIKV specific antigen labeling was detected specially in cells with few $Map2^{+}$processes (b, green). At higher viral loads of MR766 (d-f), we noticed $Map2^{low}$ and $Map2^{-}$ cells (arrows) expressing viral antigens (green).

Figure 3: **ZIKV Br infection elicits higher levels of cytokine production when compared to ZIKV 766 infection.** A detailed table of all cytokines tested can be found in the supplementary methods.

Methods

Full methods description can be found in the Supplementary Information.

Cell culture and viral infection CNS cells were harvested from swiss mouse embryos at embryo day 14 (E14) and grown as neurospheres. Neuroblastoma cells (SH-SY5Y) were cultured according to the suppliers' protocol. Cultures were tested for mycoplasma contamination once a month. Detailed information about infection can be found in the supplementary methods section.

RT-PCR NSC and SH-SY5Y were mock-infected or infected with ZIKV MR766 or ZIKV Br at MOI 0.1. Neurospheres were infected with $5x10^4$ or 10^4 PFU of each virus. Intracellular RNA were analyzed by a two-steps RT-qPCR for viral negative strand or total viral RNA with ZIKV specific primers[29].

Cytokines Supernatant from cell cultures infected with Brazilian and African ZIKV strains were collected and a multiplex biometric immunoassay was used for cytokine measurement (Bio-Plex Pro Human Cytokine - Bio-Rad).

Statistical analysis - Data are shown as mean ± s.e.m. Asterisks identify experimental groups that were significantly different from control groups by Student's t-test.

References

1 Mlakar, J. *et al.* Zika Virus Associated with Microcephaly. *The New England journal of medicine*, doi:10.1056/NEJMoa1600651 (2016).

2 Oliveira Melo, A. S. *et al.* Zika virus intrauterine infection causes fetal brain abnormality and microcephaly: tip of the iceberg? *Ultrasound in obstetrics & gynecology : the official journal of the International Society of Ultrasound in Obstetrics and Gynecology* **47**, 6-7, doi:10.1002/uog.15831 (2016).

3 Tetro, J. A. Zika and microcephaly: causation, correlation, or coincidence? *Microbes and infection / Institut Pasteur*, doi:10.1016/j.micinf.2015.12.010 (2016).

4 Cao-Lormeau, V. M. *et al.* Guillain-Barre Syndrome outbreak associated with Zika virus infection in French Polynesia: a case-control study. *Lancet (London, England)*, doi:10.1016/s0140-6736(16)00562-6 (2016).

5 Calvet, G. *et al.* Detection and sequencing of Zika virus from amniotic fluid of fetuses with microcephaly in Brazil: a case study. *The Lancet. Infectious diseases*, doi:10.1016/s1473-3099(16)00095-5 (2016).

6 Alcantara, D. & O'Driscoll, M. Congenital microcephaly. *American journal of medical genetics. Part C, Seminars in medical genetics* **166c**, 124-139, doi:10.1002/ajmg.c.31397 (2014).

7 Li, X. J. *et al.* Human Cytomegalovirus Infection Dysregulates the Localization and Stability of NICD1 and Jag1 in Neural Progenitor Cells. *Journal of virology* **89**, 6792-6804, doi:10.1128/jvi.00351-15 (2015).

8 Kumar, S. *et al.* Some observations on the tropism of Japanese encephalitis virus in rat brain. *Brain research* **1268**, 135-141, doi:10.1016/j.brainres.2009.02.051 (2009).

9 Neal, J. W. Flaviviruses are neurotropic, but how do they invade the CNS? *The Journal of infection* **69**, 203-215, doi:10.1016/j.jinf.2014.05.010 (2014).

10 Ariff, I. M., Thounaojam, M. C., Das, S. & Basu, A. Japanese encephalitis virus infection alters both neuronal and astrocytic differentiation of neural stem/progenitor cells. *Journal of neuroimmune pharmacology : the official journal of the Society on NeuroImmune Pharmacology* **8**, 664-676, doi:10.1007/s11481-013-9455-7 (2013).

11 Das, S. & Basu, A. Viral infection and neural stem/progenitor cell's fate: implications in brain development and neurological disorders. *Neurochemistry international* **59**, 357-366, doi:10.1016/j.neuint.2011.02.020 (2011).

12 Tang, H. *et al.* Zika Virus Infects Human Cortical Neural Progenitors and Attenuates Their Growth. *Cell stem cell*, doi:10.1016/j.stem.2016.02.016 (2016).

13 Kovalevich, J. & Langford, D. Considerations for the use of SH-SY5Y neuroblastoma cells in neurobiology. *Methods in molecular biology (Clifton, N.J.)* **1078**, 9-21, doi:10.1007/978-1-62703-640-5_2 (2013).

14 Chang, C. Y. *et al.* Disruption of in vitro endothelial barrier integrity by Japanese encephalitis virus-Infected astrocytes. *Glia*, doi:10.1002/glia.22857 (2015).

15 Chen, C. J. *et al.* TNF-alpha and IL-1beta mediate Japanese encephalitis virus-induced RANTES gene expression in astrocytes. *Neurochemistry international* **58**, 234-242, doi:10.1016/j.neuint.2010.12.009 (2011).

16 Das, S. *et al.* Abrogated inflammatory response promotes neurogenesis in a murine model of Japanese encephalitis. *PloS one* **6**, e17225, doi:10.1371/journal.pone.0017225 (2011).

17 Kumar, M., Verma, S. & Nerurkar, V. R. Pro-inflammatory cytokines derived from West Nile virus (WNV)-infected SK-N-SH cells mediate neuroinflammatory markers and neuronal death. *Journal of neuroinflammation* **7**, 73, doi:10.1186/1742-2094-7-73 (2010).

18 Guadagno, J., Xu, X., Karajgikar, M., Brown, A. & Cregan, S. P. Microglia-derived TNFalpha induces apoptosis in neural precursor cells via transcriptional activation of the Bcl-2 family member Puma. *Cell death & disease* **4**, e538, doi:10.1038/cddis.2013.59 (2013).

19 Thirumangalakudi, L., Yin, L., Rao, H. V. & Grammas, P. IL-8 induces expression of matrix metalloproteinases, cell cycle and pro-apoptotic proteins, and cell death in cultured neurons. *Journal of Alzheimer's disease : JAD* **11**, 305-311 (2007).

20 Lai, C. Y. *et al.* Endothelial Japanese encephalitis virus infection enhances migration and adhesion of leukocytes to brain microvascular endothelia via MEK-dependent expression of ICAM1 and the CINC and RANTES chemokines. *Journal of neurochemistry* **123**, 250-261, doi:10.1111/j.1471-4159.2012.07889.x (2012).

21 Bhowmick, S. *et al.* Induction of IP-10 (CXCL10) in astrocytes following Japanese encephalitis. *Neuroscience letters* **414**, 45-50, doi:10.1016/j.neulet.2006.11.070 (2007).

22 Wild, E. *et al.* Abnormal peripheral chemokine profile in Huntington's disease. *PLoS currents* **3**, Rrn1231, doi:10.1371/currents.RRN1231 (2011).

23 Kadota, R. *et al.* Granulocyte colony-stimulating factor (G-CSF) protects oligodendrocyte and promotes hindlimb functional recovery after spinal cord injury in rats. *PloS one* **7**, e50391, doi:10.1371/journal.pone.0050391 (2012).

24 Adepoju, A., Micali, N., Ogawa, K., Hoeppner, D. J. & McKay, R. D. FGF2 and insulin signaling converge to regulate cyclin D expression in multipotent neural stem cells. *Stem cells (Dayton, Ohio)* **32**, 770-778, doi:10.1002/stem.1575 (2014).

25 Carteaux, G. *et al.* Zika Virus Associated with Meningoencephalitis. *The New England journal of medicine*, doi:10.1056/NEJMc1602964 (2016).

26 Cauchemez, S. *et al.* Association between Zika virus and microcephaly in French Polynesia, 2013-15: a retrospective study. *Lancet (London, England)*, doi:10.1016/s0140-6736(16)00651-6 (2016).

27 Chatel-Chaix, L. *et al.* A Combined Genetic-Proteomic Approach Identifies Residues within Dengue Virus NS4B Critical for Interaction with NS3 and Viral Replication. *Journal of virology* **89**, 7170-7186, doi:10.1128/jvi.00867-15 (2015).

28 Sklan, E. H. & Glenn, J. S. in *Hepatitis C Viruses: Genomes and Molecular Biology* (ed S. L. Tan) (Horizon Bioscience Horizon Bioscience., 2006).

29 Lanciotti, R. S. *et al.* Genetic and serologic properties of Zika virus associated with an epidemic, Yap State, Micronesia, 2007. *Emerging infectious diseases* **14**, 1232-1239, doi:10.3201/eid1408.080287 (2008).

30 Johe, K. K., Hazel, T. G., Muller, T., Dugich-Djordjevic, M. M. & McKay, R. D. Single factors direct the differentiation of stem cells from the fetal and adult central nervous system. *Genes & development* **10**, 3129-3140 (1996).

Author contribution: **LC** designed and performed experiments, prepared figures and/or tables, analyzed the data, contributed with reagents/materials/analysis tools and wrote the manuscript; **AT** designed experiments, analyzed the data, contributed with reagents/materials/analysis tools and wrote the manuscript, **LH** designed and performed experiments, prepared figures and/or tables, analyzed the data and wrote the manuscript; **RD** designed and performed experiments, prepared figures and/or tables, analyzed the data and wrote the manuscript; **PP** designed and performed experiments, prepared figures and/or tables, analyzed the data and wrote the manuscript; **AV** designed and performed experiments, prepared figures and/ or tables, analyzed the data and wrote the manuscript; **GV** performed experiments; **FM** performed experiments and analyzed the data; **CV** performed experiments; **AF** contributed reagents/materials/analysis tools and analyzed the data ; **RS** designed experiments, analyzed the data and wrote the manuscript.

Acknowledgments: the author would like to thank Conselho Nacional de Desenvolvimento e Pesquisa (CNPq), Fundação de Amparo a Pesquisa do Estado do Rio de Janeiro (FAPERJ), Departamento de DST AIDS e Hepatites Virais do Ministério da Saúde do Brasil for funding research in our laboratories.

Author information The authors declare no competing financial interests. Correspondence and requests for materials should be addressed to either Amilcar Tanuri (atanuri1@gmail.com) or Loraine Campanati (lcampanati@gmail.com).

SUPPLEMENTARY INFORMATION

Methods

- **Viruses** - Brazilian ZIKV was isolated from a PCR positive, blood specimen, of an adult patient from Espirito Santo (ES), a state of southeastern Brazil during the acute phase of the disease. The African strain MR 766 was a kind gift of Dr. Davis Ferreira, UFRJ. A ZIKV protein fragment of approximately 900 pb was amplified and sequenced, confirming virus identity.

African and Brazilian ZIKV were propagated in VERO cells. Briefly, VERO cells were infected with ZIKV at a MOI = 0.01 and incubated at 37ºC. After 1 hour, inoculum was removed and cells were incubated with DMEM (Thermofisher scientific) supplemented with 2% fetal bovine serum (FBS). After 4 days, conditioned medium was harvested, cleared from dead cells and cellular drebris through centrifugation at 300 x g and sterile-filtration and stored at -80ºC.

PLAQUE ASSAY. Infectious virus particles were quantified through plaque assay. Confluent monolayers of VERO cells were inoculated with 10-fold dilution of virus stocks and samples and incubated in semisolid medium (alpha-MEM medium supplemented with 1% carboxymethylcellulose and 1% FBS) for 5 days at 37ºC. After 5 days, cells were fixed with 4% formaldehyde and stained with 1% crystal violet in 20% ethanol for plaque visualization. Virus titers represent the concentration of infectious virus particles and were expressed as plaque forming units (PFU) per milliliter.

- **Neurospheres** - cortical cells were obtained from E14 (14 days post fertilization) Swiss mouse embryos. Dissection and preparation of single cell suspensions were done according to previous work[30]. All animal procedures were done following the CEUA-CCS-UFRJ guidelines. 1 x 10^6 cells were plated on untreated 10 cm dishes (Corning) in

Neurobasal medium supplemented with B27 (Thermofisher Scientific). After 3 days, small neurospheres could already be seen floating in the medium and were harvested for the experiments. Aiming to evaluate the initiation of neurites extension of out of the neurospheres, we harvested 3 days old spheres, let them attach to PLO covered coverslips for 2 hours and immediately infected with 5x 10^4 p.f.u. of both isolates for two hours. The infection medium was then washed and replaced by fresh neurobasal medium plus B27. 48h later the area of the neurospheres was measured and extended processes analyzed, using phase contrast optics on a Nikon eclypse TE300 inverted microscope, coupled to a Leica DFC310FX camera using the LAS interactive measurements module from the LAS software (Leica Microsystems).

Neurons - 2 or 3 x10^4 E14 cells were plated onto PLO coated coverslips, in neurobasal medium supplemented with B27. After 72h, cells already presented neurite extension and showed Map2 positive staining in the control slides. Infection was made with 1 and 5 x 10^4 p.f.u. of both isolates, for two hours and the rest of the procedures was made as described above. After 48h, the cells were fixed and prepared for immunofluorescence using anti-Map2 antibody (ABCAM cat#32454; 1:1000). Images suffered minimal digital processing. Since neurites were often very thin, gamma correction was used in order to distinguish them from the background

Immunofluorescence - isolated cells and neurospheres were fixed with 4% paraformaldehyde (Sigma Aldrich) in phosphate buffered saline (PBS) for 20 minutes at room temperature. The fixative solution was removed and the samples washed 3x with PBS. Blocking of unspecific binding of the antibody and permeabilization was made with PBS + 3% bovine serum albumin (Sigma Aldrich), plus 0,1% Triton X-100 (Sigma

Aldrich) for 40 minutes at room temperature. Incubation with primary antibodies was made following manufacturers' instructions (Map2; ABCAM cat#32454; 1:1000 – Pan flavivirus antibody 4G2 http://www.atcc.org/products/all/HB-112.aspx#generalinformation). After washing 3x with PBS, cells were incubated with secondary antibodies coupled to Alexa fluorochromes (Thermofisher scientific) for 40 minutes, washed 5x and mounted with prolong gold mounting medium (Thermofisher scientific). Samples were imaged using either Leica SP5 or Leica SPE confocal microscopes and Nikon TE300 inverted microscope coupled to a Leica DFC310FX camera.

RT-PCR - NSCs and SH-SY5Y were mock infected and infected with ZIKV MR766 or ZIKV Br (both at MOI 0.1) for 3 days when cells were harvested and RNA extracted with RNeasy mini kit (Qiagen) according to manufacturer's instructions. Reverse transcription was performed with 835 forward primer for retrotranscription of viral RNA negative strand[29] or hexamers random primers for total RNA with High Capacity kit (Thermofisher scientific). Quantitative PCR (qPCR) was performed with TaqMan Universal Master Mix (Thermofisher scientific) and threshold cycle (CT) calculated for each amplification curve. Categories of CT value was determined as $30<CT<40$, $20<CT<30$ and $CT<20$. Similar infections were performed with neurospheres, except for virus concentrations that were $5x10^4$ or 10^4 total p.f.u.

Cytokines quantification - The concentration of IL-1β, IL-1ra, IL-2, IL-4, IL-5, IL-6, IL-9, IL-10, IL-12, IL-13, IL-15, IL-17a, IFNγ, TNFα, Eotaxin, IL-8, IP-10, MCP-1, MIP-1α, MIP-1β, RANTES, Basic FGF, G-CSF, GM-CSF, IL-7, PDGF and VEGF were assessed by a Bio-Plex Human 27-Plex Cytokine Panel and Reagent Kits, Bio-Rad;

according to the manufacturer's instructions. Cytokine levels were measured in cell culture supernatants of control and infected cells with ZIKV MR766 or ZIKV Br lineages at MOI 0.1, for 48h. Cytokine concentration is displayed in pg/mL and the fold change is relative to control (mock-infected cells).

Figure 1

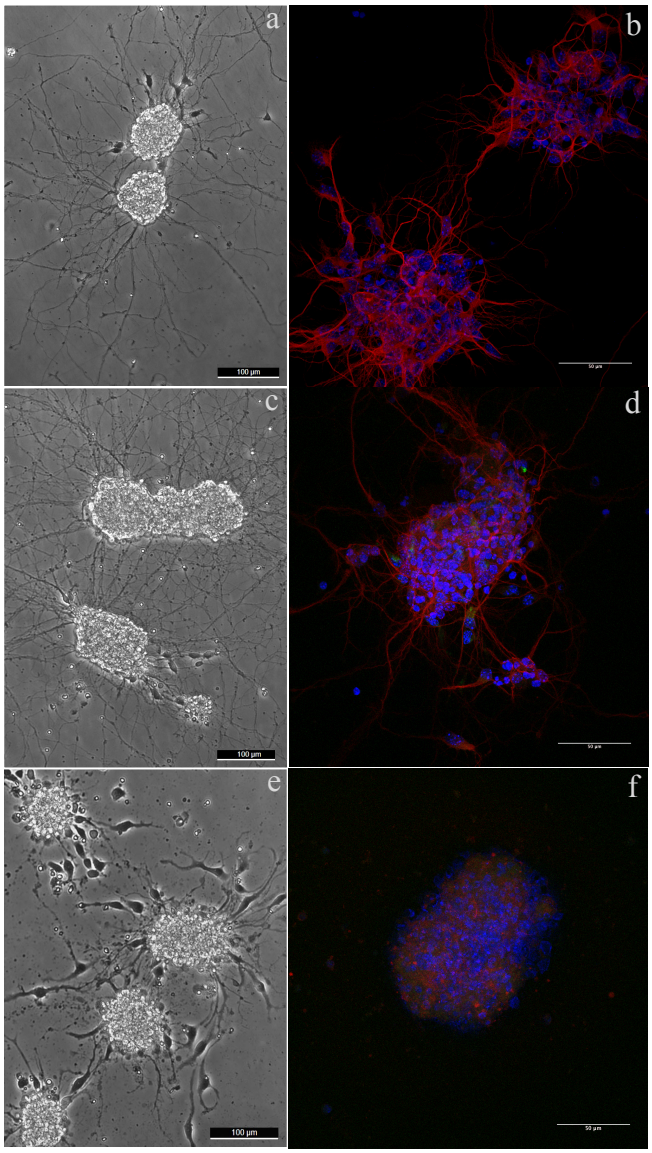
a
b
c
d
e
f
100 µm
50 µm

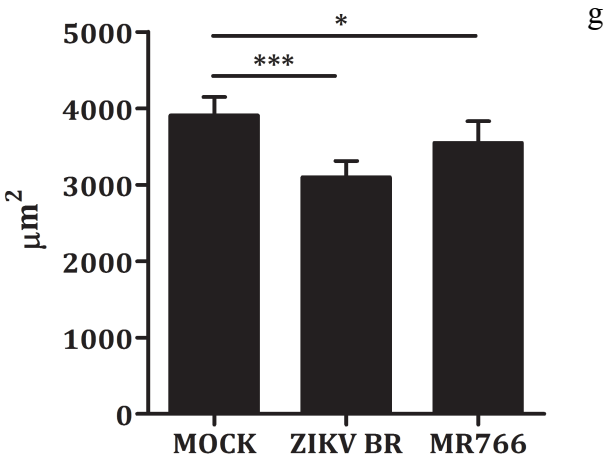
g
*
***
5000
4000
3000
2000
1000
0
µm2
MOCK
ZIKV BR
MR766

Figure 2

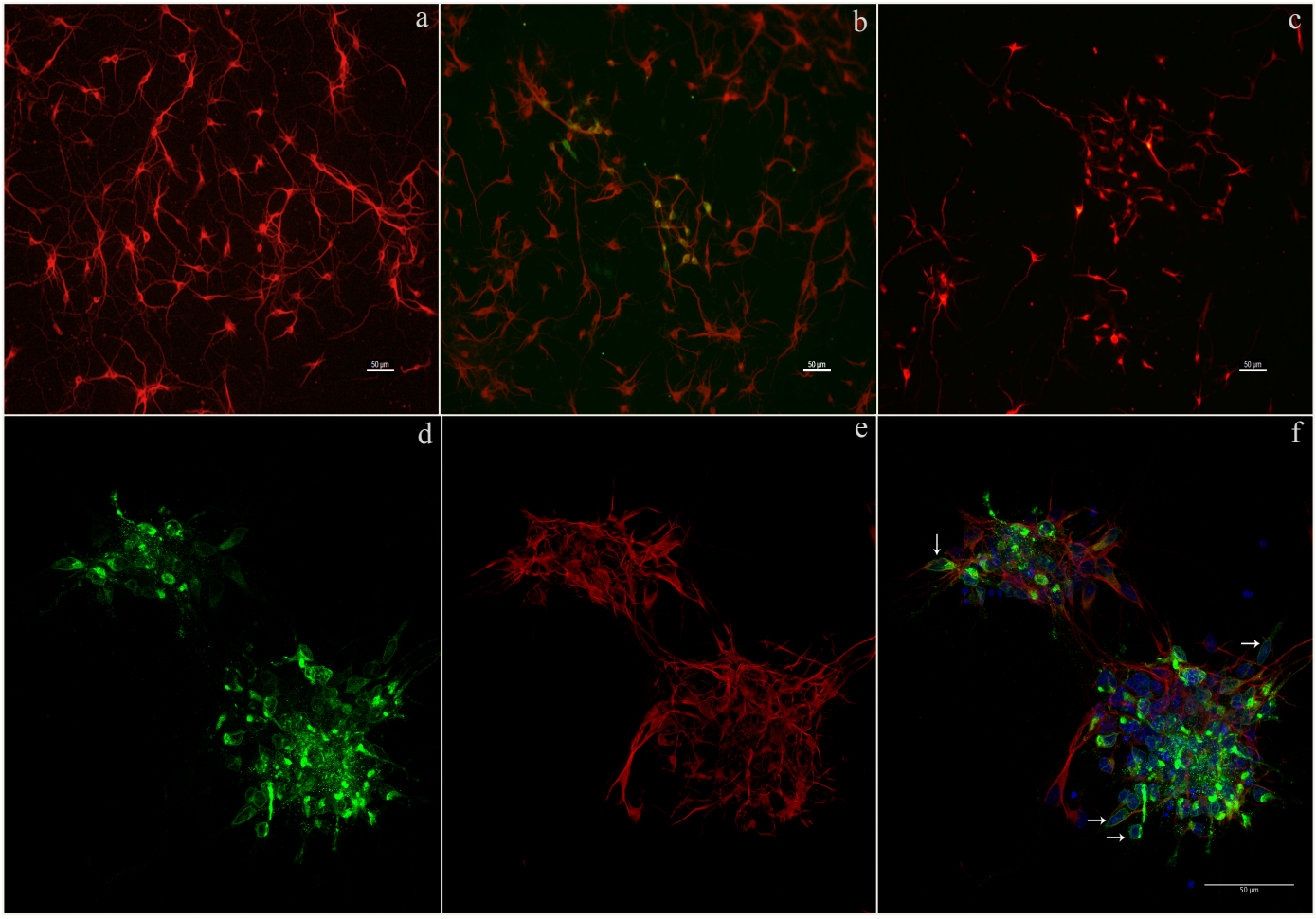

Figure 3

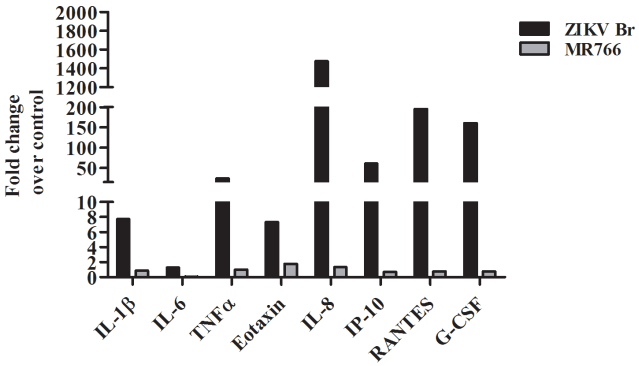

Supplementary Figure 1

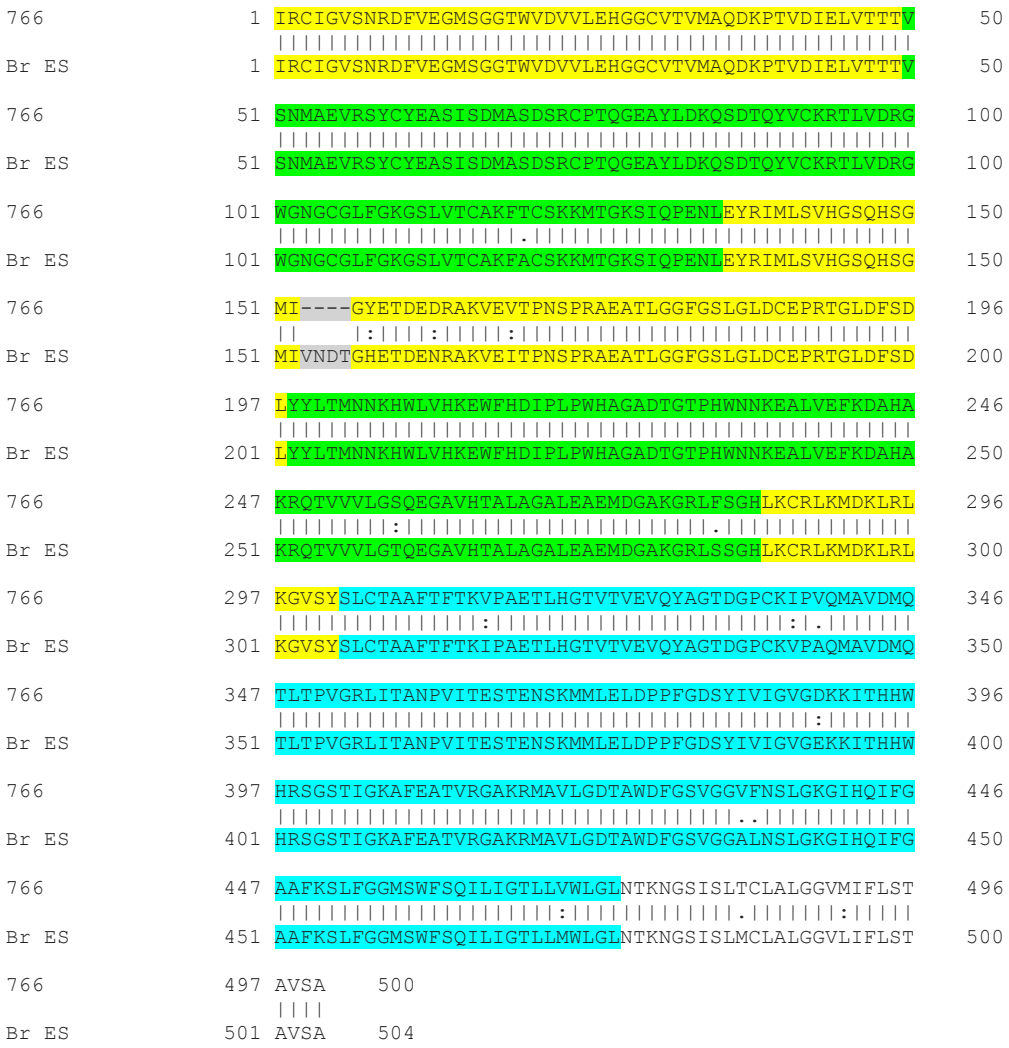

Figure S1- Amino acid alignment of ZIKV envelope sequence from African 766 (766) prototypic sequence with Brazilian (Br ES) counterpart done with *Needle* package contained in Clustal W package http://www.ebi.ac.uk/Tools/psa/emboss_needle/). Marked in yellow, green and blue are protein Domains I, II, and III, respectively. The insertion of four amino acid in BR ES Domain I is marked in gray. A vertical line between sequences represents identity and two and one points represents conservative and non-conservative substitutions, respectively. Total identity was 96.2% and similarity score was 98%.

Supplementary figure 2

```
ZIKV 766          1 NQMAIIIMVAVGLLGLITANELGWLERTKSDLSHLMGRREEGATIGFSMD     50
                    ||||||||||||||||||||||||||||:|::|||||||||||:|||||
ZIKV BR           1 NQMAIIIMVAVGLLGLITANELGWLERTKNDIAHLMGRREEGATMGFSMD     50

ZIKV 766         51 IDLRPASAWAIYAALTTFITPAVQHAVTTSYNNYSLMAMATQAGVLFGMG    100
                    |||||||||||||||.|||||||||||||||||||||||||||||||||
ZIKV BR          51 IDLRPASAWAIYAALTTLITPAVQHAVTTSYNNYSLMAMATQAGVLFGMG    100

ZIKV 766        101 KGMPFYAWDFGVPLLMIGCYSQLTPLTLIVAIILLVAHYMYLIPGLQAAA    150
                    |||||...|.||||||:|||||||||||||||||||||||||||||||||
ZIKV BR         101 KGMPFMHGDLGVPLLMMGCYSQLTPLTLIVAIILLVAHYMYLIPGLQAAA    150

ZIKV 766        151 ARAAQKRTAAGIMKNPVVDGIVVTDIDTMTIDPQVEKKMGQVLLIAVAVS    200
                    ||||||||||||||||||||||||||||||||||||||||||||||||:|
ZIKV BR         151 ARAAQKRTAAGIMKNPVVDGIVVTDIDTMTIDPQVEKKMGQVLLIAVAIS    200

ZIKV 766        201 SAILSRTAWGWGEAGALITAATSTLWEGSPNKYWNSSTATSLCNIFRGSY    250
                    ||:|.||||||||||||||||||||||||||||||||||||||||||||||
ZIKV BR         201 SAVLLRTAWGWGEAGALITAATSTLWEGSPNKYWNSSTATSLCNIFRGSY    250

ZIKV 766        251 LAGASLIYTVTRNAGLVKRR    270
                    ||||||||||||||||||||
ZIKV BR         251 LAGASLIYTVTRNAGLVKRR    270
```

Figure S2- Amino acid alignment of ZIKV NS4B sequence from African MRC 766 prototypic sequence with Brazilian (Br ES) counterpart done with *Needle* package contained in Clustal W package http://www.ebi.ac.uk/Tools/psa/emboss_needle/). Marked in yellow are five NS4B transmembrane domains. The underlined sequences represents two DNA binding sequences motifs and in bold are three important amino acids for Dengue virus replication. A vertical line between sequences represents identity and two and one points represents conservative and non-conservative substitutions, respectively. Total identity was 96.2% and similarity score was 98%.

Supplementary figure 3

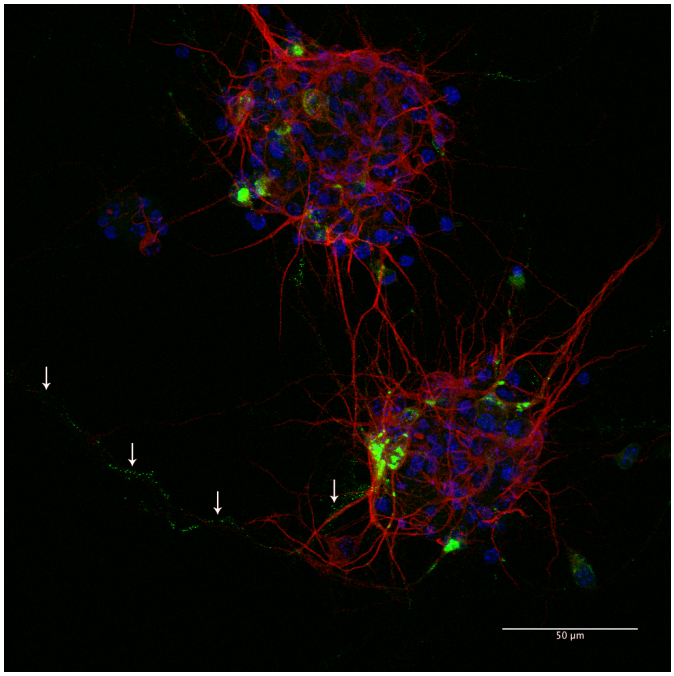

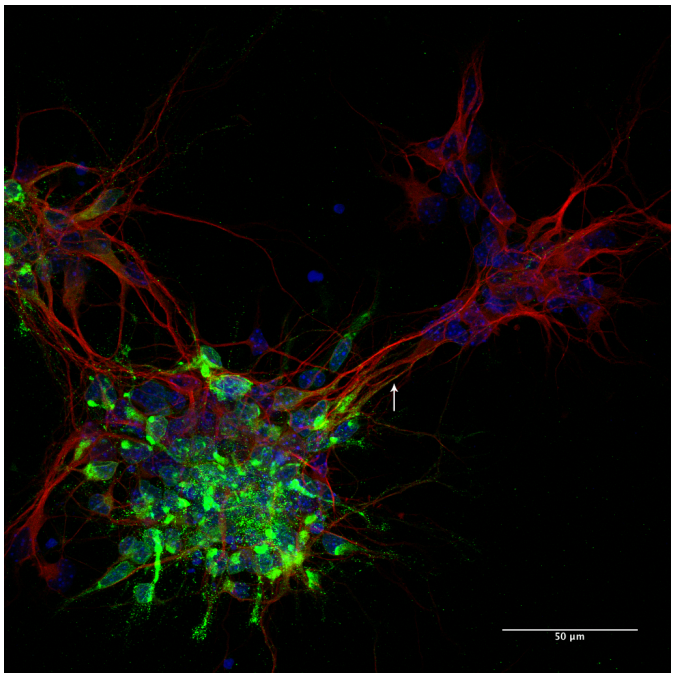

Figure S3 - Neurospheres infected with 10^6 p.f.u of ZIKV MR766 stained for Map2 (red) and flavivirus specific antigen (green). Only rarely we observed 4G2 positive neurites (arrows) growing out of the spheres.

Supplementary figure 4

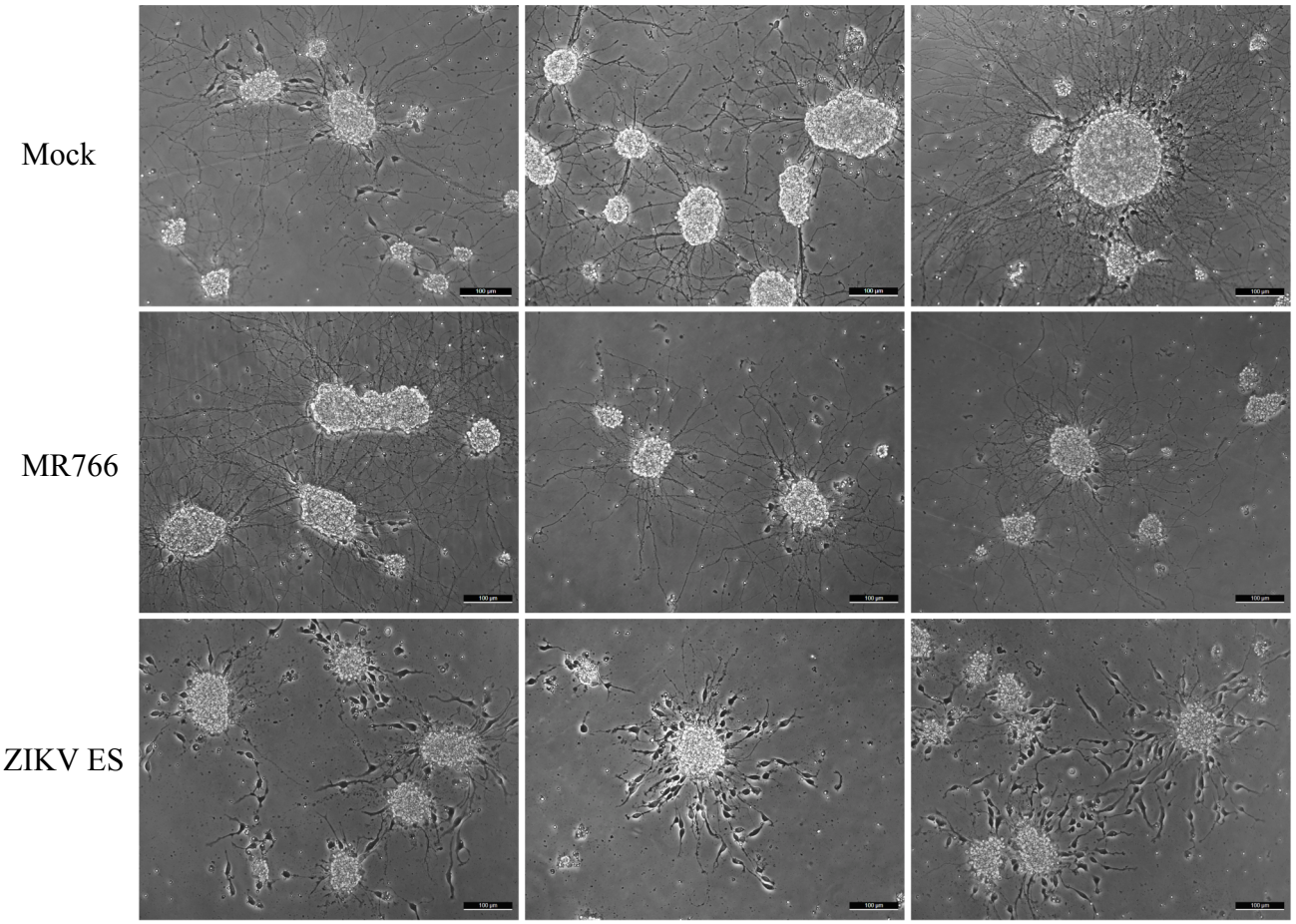

Figure S4 – More examples of infected neurospheres as seen by phase contrast microscopy.

Supplementary figure 5

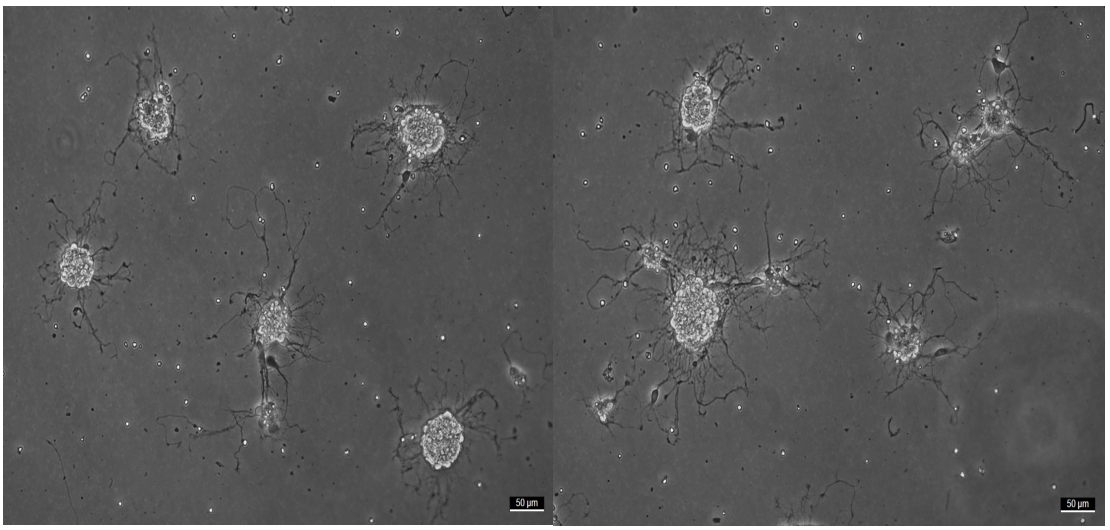

Figure S5 - Smaller neurospheres infected with MR766 had misshapen and convoluted neurites outgrowth.

Supplementary Table 1

Quantitative PCR of negative strand and total viral RNA from NSCs, SH-SY5Y and Neurosphere.

Experiment condition	NSCs☐		SH-SY5Y☐		Neurosphere*	
	RNA negative strand	Total RNA	RNA negative strand	Total RNA	RNA negative strand	Total RNA
Mock	-	-	-	-	-	-
ZIKV MR766	+	+	+++	+++	++	++
ZIKV Br	++	++	++	+++	+	+

+ 30<CT<40; ++ 20<CT<30; +++ CT<20

☐ virus infection with MOI 0.1

*virus infection with 5x104 PFU

Supplementary Table 2

Comparison of Inflammatory Cytokines, Chemokines, and Growth Factors levels in the supernatant SH-SY5Y cells (neuroblastoma cell line) after infection with Brazilian and African ZIKV lineages.

	Control	**Brazilian ZIKV (MOI 0.1)**		**African ZIKV (MR766) (MOI 0.1)**	
Analyte	pg/mL	pg/mL	Fold Change	pg/mL	Fold Change
Imflammatory Cytokines					
IL-1β	0,37	2.86	7.73	0,32	0.86
IL-1ra	28,13	135.23	4.81	21.68	0.77
IL-2	-	2,52	-	-	-
IL-4	5,09	25,48	5.01	4,82	0.95
IL-5	-	10.29	-	-	-
IL-6	8.75	11.24	1.28	0.63	0.07
IL-9	1.62	9.87	6.09	1.62	1
IL-10	39.03	47.52	1.22	37.48	0.96
IL-12	229.06	249.6	1.09	215.04	0.94
IL-13	2.98	3.74	1.26	2.84	0.95
IL-15	7.87	15.56	1.98	7.94	1.01
IL1-7a	-	20.91	-	0.77	-
IFNγ	65.15	157.16	2.41	53.9	0.83
TNFα	4.69	115.55	24.64	4.69	1.00
Chemokines					
Eotaxin	13.45	98.88	7.35	24.1	1.79
IL-8	2.98	4398.46	1475.99	4.01	1.35
IP-10	259.3	15848.65	61.12	177.77	0.69
MCP-1	1029.05	1429.51	1.39	1062.24	1.03

MIP-1α	0.39	1.66	4.26	0.26	0.67
MIP-1β	-	2,77	-	-	-
RANTES	16.03	3134.19	195.52	12.58	0.78
Growth Factors					
Basic FGF	-	16.89	-	-	-
G-CSF	2.01	322.88	160.64	1.57	0.78
GM-CSF	-	49.01	-	-	-
IL-7	59,41	70,73	1.19	61,59	1.04
PDGF	-	36,08	-	-	-
VEGF	5730.3	7383.34	1.29	4639.69	0.81

IL = interleukin; IFN- γ = interferon γ; TNF-α = tumor necrosis factor α; IP = Interferon gamma-induced protein 10; MCP = Monocyte chemoattractant protein; MIP = macrophage inflammatory protein; FGF = fibroblast growth factor; G-CSF = Granulocyte colony-stimulating factor; GM-CSF = Granulocyte-macrophage colony-stimulating factor; PDGF = Platelet Derived Growth Factor-BB; VEGF = vascular endothelial growth factor. Fold Change in cytokine level is relative of control.